Polarization effects in polymer FBGs: study and use for transverse force sensing

Xuehao Hu,[1] David Saez-Rodriguez,[2] Carlos Marques,[2] Ole Bang,[3] David J Webb,[2] Patrice Mégret,[1] and Christophe Caucheteur,[1,*]

[1]*Electromagnetism and Telecommunication Department, Université de Mons, 31 Boulevard Dolez, Mons, 7000, Belgium*

[2]*Aston Institute of Photonic Technologies, Aston University, Birmingham, B4 7ET, UK*

[3]*DTU Fotonik, Department of Photonics Engineering, Technical University of Denmark, 2800, Kgs. Lyngby, Denmark*

[*]*christophe.caucheteur@umons.ac.be*

Abstract: Bragg gratings photo-inscribed in polymer optical fibers (POFs) are more sensitive to temperature and pressure than their silica counterparts, because of their larger thermo-optic coefficient and smaller Young's modulus. Polymer optical fiber Bragg gratings (POFBGs) are most often photo-written in poly(methylmethacrylate) (PMMA) based materials using a continuous-wave 325 nm HeCd laser. In this work, we present the first study about birefringence effects in POFBGs manufactured in different types of fiber. To achieve this, highly reflective (> 90%) gratings were produced with the phase mask technique. Their spectral response was then monitored in transmission with polarized light. Polarization dependent loss (PDL) and differential group delay (DGD) were computed from the Jones matrix eigenanalysis using an optical vector analyzer. Maximum values exceeding several dB and a few picoseconds were obtained for the PDL and DGD, respectively. An inverse scattering technique applied to the experimental data provided an estimate of the photo-induced birefringence value arising from the side fabrication process. The response to lateral force was finally investigated for various incident directions using the PDL response of FBGs manufactured in step-index POFs. As the force induced birefringence adds to the photo-induced one, a force dependent evolution of the PDL maximum value was noticed, with a good temperature-insensitivity.

OCIS codes: (060.2370) Fiber optics sensors; (060.3735) Fiber Bragg gratings.

References and links

1. Z. Xiong, G. D. Peng, B. Wu, and P. L. Chu, "Highly tunable Bragg gratings in single-mode polymer optical fibers," IEEE Photon. Technol. Lett. **11**(3), 352–354 (1999).
2. D. J. Webb, K. Kalli, K. Carroll, C. Zhang, M. Komodromos, A. Argyros, M. Large, G. Emiliyanov, O. Bang, and E. Kjaer, "Recent developments of Bragg gratings in PMMA and TOPAS polymer optical fibers," Proc. SPIE **6830**, 683002 (2007).
3. G. Statkiewicz-Barabach, K. Tarnowski, D. Kowal, P. Mergo, and W. Urbanczyk, "Fabrication of multiple Bragg gratings in microstructured polymer fibers using a phase mask with several diffraction orders," Opt. Express **21**(7), 8521–8534 (2013), http://www.opticsinfobase.org/oe/abstract.cfm?URI=oe-21-7-8521.
4. H. Dobb, D. J. Webb, K. Kalli, A. Argyros, M. C. J. Large, and M. A. van Eijkelenborg, "Continuous wave ultraviolet light-induced fiber Bragg gratings in few- and single-mode microstructured polymer optical fibers," Opt. Lett. **30**(24), 3296–3298 (2005).
5. X. Chen, C. Zhang, D. J. Webb, G. D. Peng, and K. Kalli, "Bragg grating in a polymer optical fibre for strain, bend and temperature sensing," Meas. Sci. Technol. **21**(9), 094005 (2010).
6. C. A. F. Marques, L. B. Bilro, N. J. Alberto, D. J. Webb, and R. N. Nogueira, "Inscription of narrow bandwidth Bragg gratings in polymer optical fibers," J. Opt. **15**(7), 075404 (2013).

#232961 - $15.00 USD Received 21 Jan 2015; accepted 7 Feb 2015; published 12 Feb 2015

7. X. Hu, C.-F. J. Pun, H.-Y. Tam, P. Mégret, and C. Caucheteur, "Highly reflective Bragg gratings in slightly etched step-index polymer optical fiber," Opt. Express **22**(15), 18807–18817 (2014), http://www.opticsinfobase.org/oe/abstract.cfm?URI=oe-22-15-18807.
8. A. Stefani, M. Stecher, G. E. Town, and O. Bang, "Direct writing of fiber Bragg grating in microstructured polymer optical fiber," IEEE Photon. Technol. Lett. **24**(13), 1148–1150 (2012).
9. W. Yuan, A. Stefani, and O. Bang, "Tunable polymer fiber Bragg grating (FBG) inscription: fabrication of dual-FBG temperature compensated polymer optical fiber strain sensors," IEEE Photon. Technol. Lett. **24**(5), 401–403 (2012).
10. K. E. Carroll, C. Zhang, D. J. Webb, K. Kalli, A. Argyros, and M. C. J. Large, "Thermal response of Bragg gratings in PMMA microstructured optical fibers," Opt. Express **15**(14), 8844–8850 (2007), http://www.opticsinfobase.org/oe/abstract.cfm?URI=oe-15-14-8844.
11. H. Y. Liu, G. D. Peng, and P. L. Chu, "Thermal tuning of polymer optical fiber Bragg gratings," Photon. Technol. Lett. **13**(8), 824–826 (2001).
12. W. Yuan, A. Stefani, M. Bache, T. Jacobsen, B. Rose, N. Herholdt-Rasmussen, F. K. Nielsen, S. Andresen, O. B. Sørensen, K. S. Hansen, and O. Bang, "Improved thermal and strain performance of annealed polymer optical fiber Bragg gratings," Opt. Commun. **284**(1), 176–182 (2011).
13. Z. F. Zhang, C. Zhang, X. M. Tao, G. F. Wang, and G. D. Peng, "Inscription of polymer optical fiber Bragg grating at 962 nm and its potential in strain sensing," IEEE Photon. Technol. Lett. **22**(21), 1562–1564 (2010).
14. W. Yuan, L. Khan, D. J. Webb, K. Kalli, H. K. Rasmussen, A. Stefani, and O. Bang, "Humidity insensitive TOPAS polymer fiber Bragg grating sensor," Opt. Express **19**(20), 19731–19739 (2011), http://www.opticsinfobase.org/oe/abstract.cfm?URI=oe-19-20-19731.
15. C. Markos, A. Stefani, K. Nielsen, H. K. Rasmussen, W. Yuan, and O. Bang, "High-T_g TOPAS microstructured polymer optical fiber for fiber Bragg grating strain sensing at 110 degrees," Opt. Express **21**(4), 4758–4765 (2013), http://www.opticsinfobase.org/oe/abstract.cfm?URI=oe-21-4-4758.
16. I. P. Johnson, W. Yuan, A. Stefani, K. Nielsen, H. Rasmussen, L. Khan, D. J. Webb, K. Kalli, and O. Bang, "Optical fibre Bragg grating recorded in TOPAS cyclic olefin copolymer," Electron. Lett. **47**(4), 271–272 (2011).
17. H. Y. Liu, H. B. Liu, G. D. Peng, and P. L. Chu, "Observation of type I and type II gratings behavior in polymer optical fiber," Opt. Commun. **220**(4-6), 337–343 (2003).
18. H. B. Liu, H. Y. Liu, G. D. Peng, and P. L. Chu, "Novel growth behaviors of fiber Bragg gratings in polymer optical fiber under UV irradiation with low power," Photon. Technol. Lett. **16**(1), 159–161 (2004).
19. D. Sáez-Rodríguez, K. Nielsen, H. K. Rasmussen, O. Bang, and D. J. Webb, "Highly photosensitive polymethyl methacrylate microstructured polymer optical fiber with doped core," Opt. Lett. **38**(19), 3769–3772 (2013).
20. W. Zhang and D. J. Webb, "Humidity responsivity of poly(methyl methacrylate)-based optical fiber Bragg grating sensors," Opt. Lett. **39**(10), 3026–3029 (2014).
21. W. Zhang, D. J. Webb, and G. Peng, "Polymer optical fiber Bragg grating acting as an intrinsic biochemical concentration sensor," Opt. Lett. **37**(8), 1370–1372 (2012).
22. C. Zhang, X. Chen, D. J. Webb, and G. D. Peng, "Water detection in jet fuel using a polymer optical fibre Bragg grating," Proc. SPIE **7503**, 750380 (2009).
23. N. Belhadj, S. Larochelle, and K. Dossou, "Form birefringence in UV-exposed photosensitive fibers computed using a higher order finite element method," Opt. Express **12**(8), 1720–1726 (2004), http://www.opticsinfobase.org/oe/abstract.cfm?URI=oe-12-8-1720.
24. T. Erdogan and V. Mizrahi, "Characterization of UV-induced birefringence in photosensitive Ge-doped silica optical fibers," J. Opt. Soc. Am. B **11**(10), 2100–2105 (1994).
25. C. Caucheteur, S. Bette, R. Garcia-Olcina, M. Wuilpart, S. Sales, J. Capmany, and P. Mégret, "Influence of the grating parameters on the polarization properties of fiber Bragg gratings," J. Lightwave Technol. **27**(8), 1000–1010 (2009).
26. C. Caucheteur, S. Bette, R. Garcia-Olcina, M. Wuilpart, S. Sales, J. Capmany, and P. Mégret, "Transverse strain measurements using the birefringence effect in fiber Bragg gratings," IEEE Photon. Technol. Lett. **19**(13), 966–968 (2007).
27. B. T. Kuhlmey, R. C. McPhedran, and C. Martijn de Sterke, "Modal cutoff in microstructured optical fibers," Opt. Lett. **27**(19), 1684–1686 (2002).
28. D. Sáez-Rodríguez, K. Nielsen, H. K. Rasmussen, O. Bang, and D. J. Webb, "Highly photosensitive polymethyl methacrylate microstructured polymer optical fiber with doped core," Opt. Lett. **38**(19), 3769–3772 (2013).
29. X. Hu, C. F. Pun, H. Y. Tam, P. Mégret, and C. Caucheteur, "Tilted Bragg gratings in step-index polymer optical fiber," Opt. Lett. **39**(24), 6835–6838 (2014).
30. S. Bette, C. Caucheteur, M. Wuilpart, P. Mégret, R. Garcia-Olcina, S. Sales, and J. Capmany, "Spectral characterization of differential group delay in uniform fiber Bragg gratings," Opt. Express **13**(25), 9954–9960 (2005), http://www.opticsinfobase.org/oe/abstract.cfm?URI=oe-13-25-9954.
31. F. Lhommé, C. Caucheteur, K. Chah, M. Blondel, and P. Mégret, "Synthesis of fiber Bragg grating parameters from experimental reflectivity: a simplex approach and its application to the determination of temperature-dependent properties," Appl. Opt. **44**(4), 493–497 (2005).
32. E. Chehura, C.-C. Ye, S. E. Staines, S. W. James, and R. P. Tatam, "Characterization of the response of fibre Bragg gratings fabricated in stress and geometrically induced high birefringence fibres to temperature and transverse load," Smart Mater. Struct. **13**(4), 888–895 (2004).

#232961 - $15.00 USD Received 21 Jan 2015; accepted 7 Feb 2015; published 12 Feb 2015

33. K. Chah, D. Kinet, M. Wuilpart, P. Mégret, and C. Caucheteur, "Femtosecond-laser-induced highly birefringent Bragg gratings in standard optical fiber," Opt. Lett. **38**(4), 594–596 (2013).
34. Y. Wang, M. Wang, and X. Huang, "High-sensitivity fiber Bragg grating transverse force sensor based on centroid measurement of polarization-dependent loss," Meas. Sci. Technol. **21**(6), 065304 (2010).
35. T. Geernaert, G. Luyckx, E. Voet, T. Nasilowski, K. Chah, M. Becker, H. Bartelt, W. Urbanczyk, J. Wojcik, W. De Waele, J. Degrieck, H. Terryn, F. Berghmans, and H. Thienpont, "Transversal load sensing with fiber Bragg gratings in microstructured optical fibers," Phot. Technol. Lett. **21**(1), 6–8 (2009).
36. S. C. Rashleigh and M. J. Marrone, "Temperature dependence of stress birefringence in an elliptically clad fiber," Opt. Lett. **8**(2), 127–129 (1983).

1. Introduction

Fiber Bragg gratings (FBGs) were first photo-inscribed in polymer optical fibers (POFs) in the late nineties [1]. Since then, strong progress has been made and polymer optical FBGs (POFBGs) are now routinely manufactured, mainly using the phase-mask technique, either under static exposition [2–4] or with a laser beam scanning along the fiber axis [5–7]. Besides, the point-by-point technique has also been exploited to produce fourth order gratings [8]. POFBGs present several attractive features for sensing purposes. Compared to their counterparts produced in silica fibers, they are more sensitive to temperature and pressure because of the larger thermo-optic coefficient and smaller Young's modulus of polymer materials [8–13]. While different polymer materials can be used to manufacture POFs [14–19], poly(methyl methacrylate) (PMMA) is the most often encountered one. PMMA demonstrates absorption of moisture up to 2 w.t. %, so that PMMA FBGs can be used as humidity sensors [20], biochemical concentration sensors [21] or water detection sensors [22].

In this paper, we study for the first time birefringence effects in highly reflective POFBGs, allowing us to use them for temperature-insensitive transverse force sensing. In practice, birefringence arises from both the lateral inscription process and the application of a transverse force. Indeed, like in silica fiber, the exposition of a single side of a POF to an incident laser beam induces a small quantity of photo-induced birefringence that combines with the intrinsic fiber birefringence and leads to polarization effects within the grating [23]. The birefringence causes the orthogonal polarization modes (so-called eigenmodes) to experience different couplings through the grating [24]. The resulting transmitted spectrum is then the combination of two overlapping spectra, offset in wavelength by typically a few picometers but otherwise identical. Birefringence is revealed by the fiber's polarization properties, such as polarization dependent loss (PDL) and differential group delay (DGD). Their maximum values depend on the grating physical parameters and on the birefringence value and can reach several dB and several tens of picoseconds, respectively [25]. These properties impair data transmission at high bitrates but they can be advantageously exploited for transverse force sensing, yielding intrinsic temperature-insensitivity [26]. In this work, they were both computed from the Jones matrix eigenanalysis method using an optical vector analyzer (OVA CTe from Luna Technologies). For this, POFBGs were UV-glued to silica fibers for measurement in transmission with polarized light. The photo-induced birefringence resulting from the side inscription process was estimated for three types of POFs (step-index, microstructured and high-birefringence microstructured) thanks to a numerical adjustment of the experimental curves by an inverse scattering program. The purpose here is not to study the effect of the writing parameters (laser power, inscription time, fluence, etc) on the birefringence value but rather to figure out, for standard inscriptions parameters, what is the degree of birefringence typically induced by the side writing process. We show that it can reach 10^{-6}-10^{-5}, depending on the fiber type.

Finally, the response to lateral force was investigated for gratings written in step-index POFs. Since transverse forces induce mechanical birefringence in addition to the photo-induced one, a drastic change of the PDL was noticed, depending on the orientation of the transverse force with respect to the FBG eigenmodes. A maximum sensitivity of 2.5 dB/N was reached, which can be readily measured. In our experiments, we focus on small

#232961 - $15.00 USD Received 21 Jan 2015; accepted 7 Feb 2015; published 12 Feb 2015

transverse force values, for which the FBGs eigenmodes overlap and cannot be easily processed to find the birefringence value from their wavelength separation.

This first study on birefringence effects in POFBGs paves the way to further sensor developments (magnetic field or current sensing, plasmonic generation with fiber gratings, etc…) where the monitoring of polarization properties bring a superior sensitivity compared to classical read-out techniques.

2. Fiber characteristics and FBGs photo-inscription

Three types of PMMA-based POFs were used in this work, as shown in Fig. 1. Step-index POFs were supplied by the *Hong Kong Polytechnic University*. The cladding (diameter: 150 µm) is in pure PMMA while the core (diameter: 8.2 µm) is composed of PMMA doped with diphenyl sulfide (5% mole) and trans-4-stilbenemethanol (1% w.t.). Microstructured POFs (mPOFs) were produced at the *Technical University of Denmark* using undoped PMMA with a hexagonal structure of three rings in the inner cladding. The hole diameter is d = 1.87 µm while the pitch is Λ = 4.26 µm and the fiber has a diameter of 135 µm. This means that the mPOF has a relative hole diameter of d/Λ = 0.44 and is endlessly single-moded [27]. High-birefringence mPOFs (diameter ~400 µm) were also investigated. They were purchased from *Kiriama*, Australia. As depicted in Fig. 1(c), there are two very large holes in the microstructured region of this fiber and a tiny bridge of PMMA between them. This bridge is so narrow that it does not permit light propagation. As a result, the modes are localized at both ends of the bridge where its thickness is greater. The diameter of the small holes in the microstructured cladding vary in the fiber cross-section in the range of 2-6 µm. Large holes have elliptical shape with axes measuring 14 × 17.5 µm and the separation between the centers of the cores is about 11 µm.

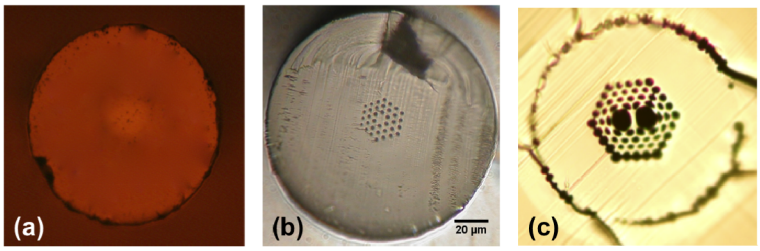

Fig. 1. Cross-section images of POFs used in this work: (a) step-index PMMA POF, (b) microstructured PMMA POF and (c) highly birefringent microstructured PMMA POF (zoom around the fiber center).

5-6 mm long FBGs with high reflectivity were photo-inscribed with a helium-cadmium laser emitting at 325 nm with the scanning phase mask technique, using the set-ups described in [28,29]. Step-index POFBGs were manufactured at the *University of Mons* using a He-Cd laser Kimmon IK5751I-G with an output power of 30 mW at 325 nm and a beam width of 1.2 mm. mPOFBGs were fabricated at *Aston University* using a He-Cd laser Kimmon IK3301R-G with similar characteristics.

POF sections were then UV-glued (Norland 78) at both sides of the grating with 8° angled silica fiber connectors for measurement in transmission. The index matching UV-glue prevents Fabry-Perot cavity effects while angled connectors avoid unwanted Fresnel reflections. To obtain measurements in transmission with polarized light, we have used an optical vector analyzer (OVA CTe from Luna Technologies), offering both a high wavelength resolution (1.25 pm) and fast scanning rate (less than 1 s to analyze a range of a few tens of nm). The PDL and DGD curves were computed from the Jones matrix using the eigenanalysis, as done in [26,30]. Gratings and connecting fibers were secured to avoid unwanted polarization fluctuations.

#232961 - $15.00 USD Received 21 Jan 2015; accepted 7 Feb 2015; published 12 Feb 2015

The photo-induced birefringence value was then estimated through a numerical fit of the experimental evolutions, using an in-house developed inverse scattering program based on the Nelder-Mead simplex algorithm [31]. The transmitted amplitude spectrum was first adjusted to get the FBG physical parameters (length, grating period and refractive index modulation). Note that the two former were *a priori* known from the writing process. With these values, the PDL and DGD curve were reconstructed and the birefringence value was optimized to minimize the difference between experimental and simulated evolutions.

3. Photo-induced birefringence in UV-induced FBGs

3.1 Step-index POFBGs

Figure 2 depicts the insertion loss, PDL and DGD spectra (blue curves) of a 6 mm long FBG written in the step-index POF measured by the OVA. The scanning rate of the laser beam along the phase mask axis was 3 µm/s. By measuring the transmitted amplitude spectrum, the maximum reflectivity has been computed to be 97%. The maximum value of PDL is equal to 0.9 dB above the noise level. Out of the rejection band, the PDL should lie around 0 dB. The latter is close to 0.8 dB, which is essentially due to the splices. As for uniform FBGs written in silica fiber, the PDL spectra exhibit two main peaks of nearly equal amplitude. They appear at wavelengths corresponding to the edges of the rejection band. Indeed, it has been shown that for FBGs, the PDL is equal to the ratio of the two grating eigenmodes [26]. Hence, the PDL is minimum at the Bragg wavelength (where both x and y spectra are equal) and maximum at the edges (where the difference in amplitude between the x and y spectra is the maximum). Similar to gratings produced in silica fibers [30], the DGD curve exhibits four main peaks. The maximum value of DGD is 3.3 ps above noise level.

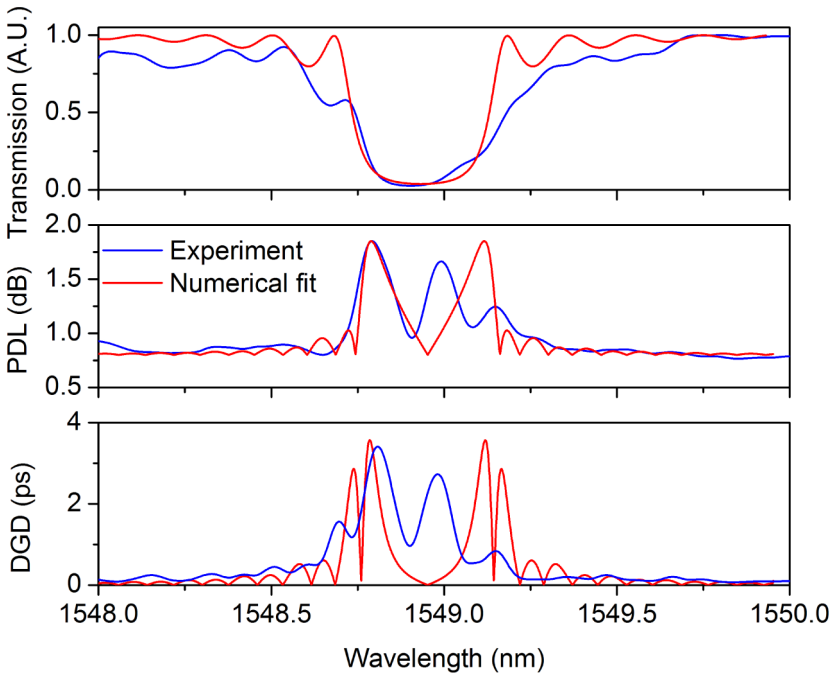

Fig. 2. Transmitted spectrum, PDL and DGD for a 6 mm long step-index POFBG: experimental profiles (blue curves) and numerical fit (red curves).

Figure 2 also depicts the numerically reconstructed spectra (red curves) and confirms a relatively good agreement with the experimental curves. It is worth mentioning that the non-zero PDL value outside of the rejection band has been taken into account in the reconstruction

#232961 - $15.00 USD Received 21 Jan 2015; accepted 7 Feb 2015; published 12 Feb 2015

process as an extra PDL value, which is not attributed to the photo-writing process. A discrepancy between experimental and simulated spectra is noticed mainly for the right-hand PDL and DGD peaks, which is attributed to the spectral deformation of the rejection band on that side. The numerical reconstruction yields a birefringence value estimated to $7.2 \times 10^{-6} \pm 0.5 \times 10^{-6}$.

3.2 mPOFBGs

Similar measurements were conducted for the two types of mPOFBGs used in this work. Figure 3 depicts the transmitted spectrum, PDL and DGD curves of a 91% reflective grating (5 mm in length) manufactured in the regular endlessly single-mode mPOF depicted in Fig. 1(b). Here, the maximum values of PDL and DGD are 4.8 dB and 9 ps above noise level, respectively, showing that photo-induced birefringence is also present for this mPOF, with an even higher value than for step-index POFs. It is worth mentioning that the irregular evolution at the left side was observed for highly reflective gratings only. The inset of Fig. 3 shows the reflected spectrum of a slightly reflective grating, without asymmetric response. The spectrum degeneracy rises with the reflectivity and is attributed to the concentration of the refractive index modulation to one side of the fiber cross-section, rather than being symmetrical about the center axis. The numerical adjustment of the main resonance (red curves) was conducted as explained above and yields a birefringence value estimated to be $3.0 \times 10^{-5} \pm 0.1 \times 10^{-5}$. This higher value (~4-fold enhancement compared to step-index POF) is attributed to the microstructured nature of the fiber, which creates more photo-induced defects during the UV illumination and consequently induces more form birefringence.

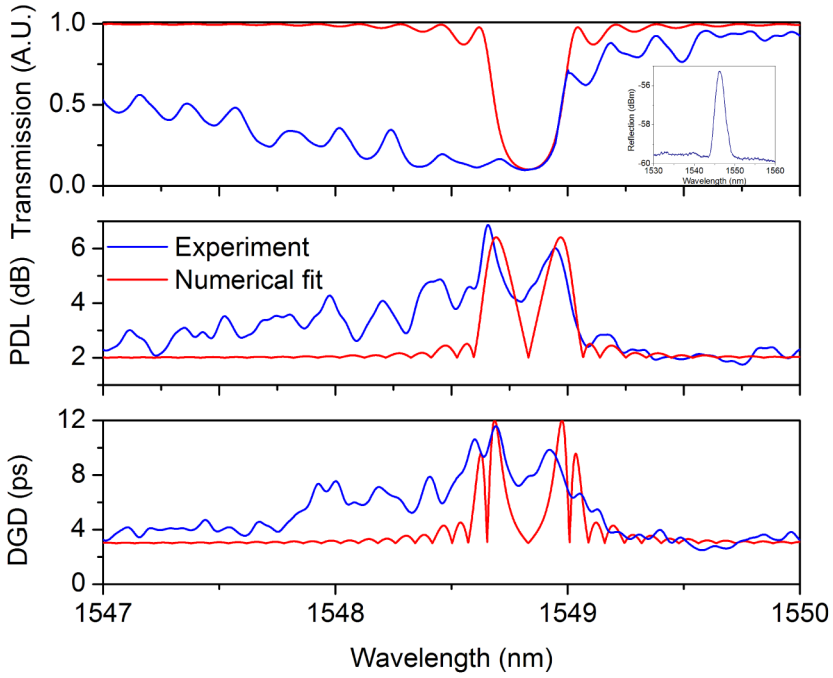

Fig. 3. Transmitted spectrum, PDL and DGD for a 5 mm long mPOFBG: experimental evolutions (blue curves) and numerical fit (red curves).

Finally, polarization measurements were also conducted for gratings manufactured in the high-birefringence mPOF depicted in Fig. 1(c). Here, the pristine fiber birefringence is such that both orthogonal polarization modes are sufficiently spaced for reliable measurement with polarized light. Figure 4 depicts the insertion loss of a 5 mm long FBG corresponding to the

#232961 - $15.00 USD Received 21 Jan 2015; accepted 7 Feb 2015; published 12 Feb 2015

slow and fast axes of the mPOF as well as the corresponding PDL curve. The wavelength separation between both peaks (which corresponds to $2\Delta n\Lambda$ where Δn is the birefringence value and Λ the grating period) has been computed to be equal to 910 pm. It yields a birefringence equal to 8×10^{-4}, which is typical for polarization maintaining optical fibers.

Measurements have been conducted on other gratings, displaying similar birefringence values as the ones reported above. Hence, these results reveal that standard photo-inscription parameters yield significant photo-induced birefringence in PMMA, which further depends on the fiber morphology.

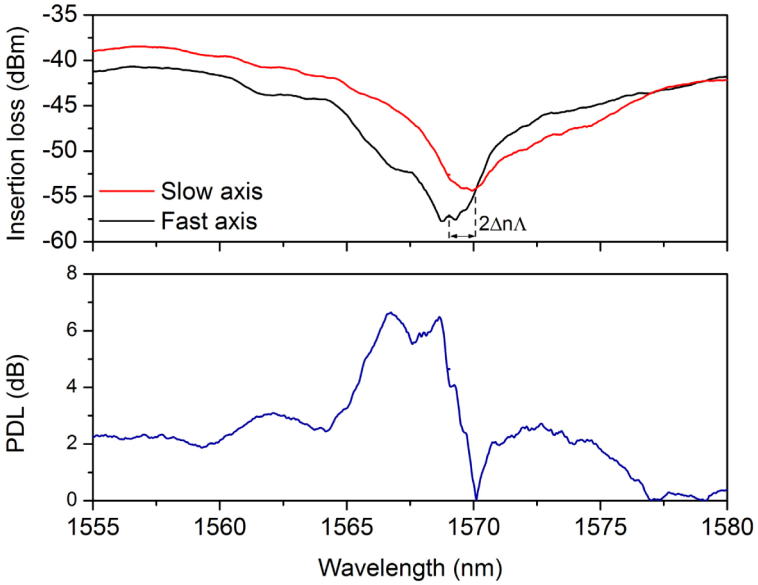

Fig. 4. Orthogonally-polarized insertion loss and PDL for a 5 mm long FBG in highly birefringent mPOF.

4. Transverse force measurement with step-index POFBGs

It is known that a transverse force brings linear birefringence, which is spectrally manifested by an increase of the PDL and DGD maximum values, up to saturation [26]. The saturation is obtained for birefringence values such that the orthogonally-polarized rejection band do not overlap anymore. In the following, we make use of the PDL curve for transverse force sensing purposes. We focus in practice on small transverse force values, for which the transmitted amplitude spectra cannot be reliably used to evaluate the birefringence value, due to the strong overlap between the orthogonally-polarized spectra. The experimental set-up used to load the optical fiber is sketched in Fig. 5. It is similar to those used in [32,33]. Two step-index POFs with and without grating, respectively, were placed parallel and pressed between two 20 mm long metal plates, which avoided the tilt of the loading area. The loads were applied and varied on the top of the plate. We focus on small transverse force values to highlight the influence of the force direction with respect to the grating eigenmodes on the sensitivity. For this, the fiber containing the FBG was oriented thanks to a pair of rotative clamps from 0° to 360° by step of 15°. The 0° direction roughly corresponds to the plane perpendicular to the laser incidence plane during the photo-inscription (the later was identified by tapes placed on the POF sample, at each side of the FBG). For each angle, measurements were done for increasing and decreasing transverse force values in the range [0-0.75N]. The PDL maximum value was then computed as a function of the transverse force value.

#232961 - $15.00 USD Received 21 Jan 2015; accepted 7 Feb 2015; published 12 Feb 2015

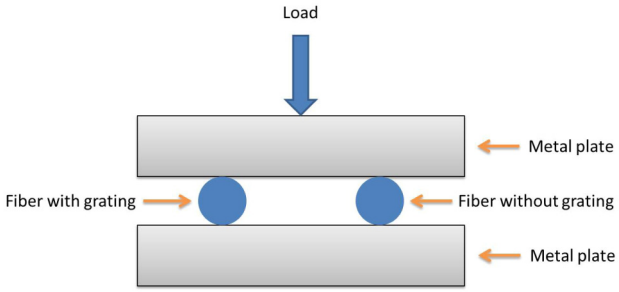

Fig. 5. Sketch of the experimental set-up used for transverse force test.

Figure 6 depicts the evolution of the PDL maximum value for a 6 mm long FBG as a function of the transverse force for two orthogonal orientations yielding opposite behaviors, namely 90° and 180°. At 90°, the PDL is linearly increasing, as the transverse force direction coincides with the laser incidence plane, resulting in birefringence increase. The opposite trend is obtained at 180°, where the form birefringence created by the transverse force value in the investigated range compensates the photo-induced birefringence. The sensitivities obtained for increasing and decreasing transverse force values are quite similar. A linear regression of the raw data yields a maximum PDL value sensitivity equal to 1.70 dB/N ± 0.20 dB/N and a minimum one equal to - 0.27 ± 0.08 dB/N. The standard deviation on the measured PDL value for each force measurement is equal to ~0.05 dB and is caused by the fluctuations of the OVA.

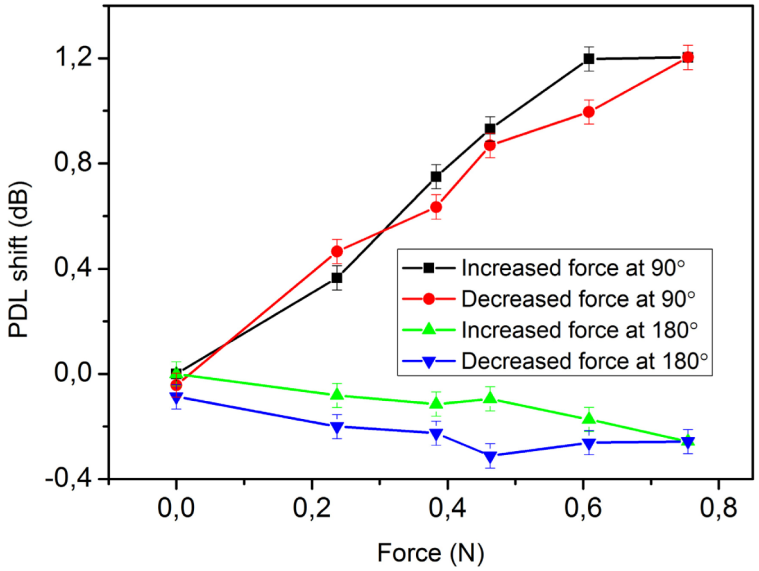

Fig. 6. Change of the maximum PDL amplitude for increasing and decreasing transverse force values applied along the two directions providing opposite behaviors.

Figure 7 further highlights the effect of the transverse force orientation on the sensor sensitivity. To obtain this figure, the load was gradually applied and the spectra simultaneously monitored for each fiber orientation with respect to the transverse force direction. The different sensitivities were then computed by a linear regression, as shown in Fig. 6. As expected due to the limited investigated range of transverse force values [34,35], the sensitivity shows an angular dependence versus the relative orientation of the optical fiber, with a periodicity equal to 180°. The maximum values are obtained for the 90° and 270°

#232961 - $15.00 USD Received 21 Jan 2015; accepted 7 Feb 2015; published 12 Feb 2015

orientations. They are equal to 1.75 dB/N and 2.57 dB/N, respectively. A difference of sensitivity (40%) is obtained between the two extrema. As illustrated in Fig. 6, it is attributed to the side writing process that leads to a stronger change of the refractive index for the fiber side facing the UV laser than for the opposite side. The maximum sensitivity is obtained when the load direction perfectly coincides with the laser incidence.

Obviously, for force values above a few Newton, a positive slope in the PDL shift versus force is obtained whatever the force orientation. It results from the fact that the mechanically-induced birefringence is always higher than the photo-induced one. However, in this case, the wavelength splitting between orthogonal polarization modes is such that the measurement can be based on its monitoring and the PDL (or DGD) spectrum does no longer bring a superior sensitivity.

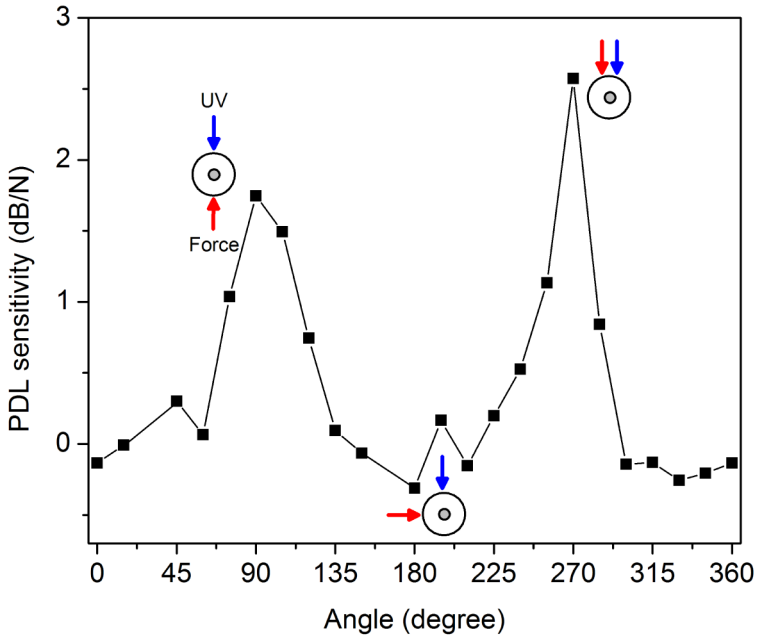

Fig. 7. Sensitivity of PDL shift versus transverse force in the range 0°-360° for a 6 mm long FBG in step-index POF. The sketches show the relative orientation of the applied force with respect to the laser incidence.

Finally, the temperature influence on the PDL maximum value was investigated for the step-index POFBG used above. It was placed inside an oven whose temperature can be controlled with an accuracy of 0.1 °C. The maximum temperature investigated in this work was 45 °C. Figure 8 demonstrates that the PDL value varies slightly with temperature for the unloaded POFBG. A linear regression yields a sensitivity of only - 0.007 dB/ °C with an uncertainty of 0.008 dB/°C, which is in good agreement with the previous works conducted on silica fibers [26,36]. Hence, temperature-insensitive measurements are possible with such sensors.

#232961 - $15.00 USD Received 21 Jan 2015; accepted 7 Feb 2015; published 12 Feb 2015

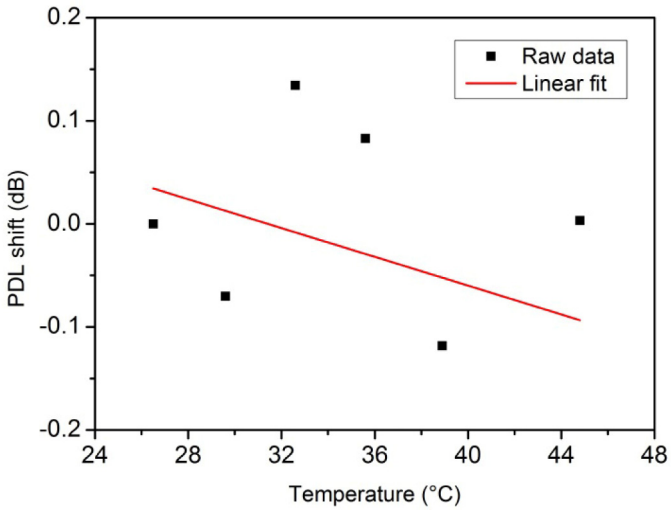

Fig. 8. PDL amplitude variation versus temperature in the range [25-45 °C].

5. Conclusion

In this work, we have used highly reflective FBGs written in PMMA-based POFs to investigate photo-induced birefringence effects arising from a standard fabrication process based on the use of a UV He-Cd laser emitting at 325 nm. The photo-induced birefringence was estimated from a numerical reconstruction of the polarization dependent loss and differential group delay spectra using an inverse scattering method. For step-index POFs, photo-induced birefringence effects are comparable to those obtained in silica fibers. They are superior in microstructured POFs, essentially due to their morphology that makes local birefringence effects more susceptible to happen during the side illumination process. Finally, the response to lateral force was investigated by measuring the maximum PDL evolution of step-index POFBGs. For small force values, it was demonstrated that the sensitivity depends on the relative angle between the photo-induced birefringence axis and the transverse force direction, which induces mechanical birefringence. A maximum sensitivity of 2.57 dB/N has been obtained, with a good temperature-insensitivity (< 3% error for a 10 °C variation). This first study of birefringence effects (both photo-induced and mechanically-induced) in POFBGs paves the way to other sensor developments, in various fields such as the measurement of magnetic field or current, plasmonic generation with metal-coated gratings, etc. No doubt that in these fields, the metrology of the FBG's polarization properties will bring a superior sensitivity compared to standard measurement techniques based on the recording of the amplitude spectrum.

Acknowledgments

This research has been conducted in the frame of the ERC (European Research Council) *Starting Grant* PROSPER (grant agreement N° 280161 – http://www.umons.ac.be/erc-prosper) and the ARC research programme PREDICTION supported by the Ministère de la Communauté française de Belgique. C. Caucheteur is supported by the F.R.S.-FNRS. This work was partially supported by Marie Curie Intra European Fellowships included in the 7th Framework Program of the European Union (projects PIEF-GA-2011-302919 and PIEF-GA-2013-628604). Authors gratefully thank Professor Tam from *Hong Kong Polytechnic Institute* for providing the optical fiber used in this work. Part of the research leading to these results has received funding from the People Programme (Marie Curie Actions) of the European Union's Seventh Framework Programme FP7/2007-2013/ under REA grant agreement n° 608382.